

3-D Tennis Ball Trajectory Estimation from Multi-view Videos and Its Parameterization by Parabola Fitting

Kenta Sohara^a and Yasuyuki Sugaya^b

Toyohashi University of Technology, Toyohashi, Aichi, Japan

Keywords: 3-D Reconstruction, Multi-views, Parabola Fitting, Parameterization of Ball Trajectory.

Abstract: We propose a new method for estimating 3-D trajectories of a tennis ball from multiple video sequences and parameterizing the 3-D trajectories. We extract candidate positions of a ball by a frame difference technique and reconstruct 3-D positions of them by two-view reconstruction for every image pairs. By analyzing a distribution of the reconstructed 3-D points, we find a cluster among them and decide its cluster center as the 3-D ball position. Moreover, we fit a plane to the estimated 3-D trajectory and express them as a 2-D point data. We parameterize the 2-D data by fitting two parabolas to them. By simulation and real experiments, we demonstrate the efficiency of our method.

1 INTRODUCTION

Recently, computer vision techniques have attracted a lot of attention in sports analytics. For example, in order to improve player skills, one analyzes sports scenes by using computer vision techniques. For judging and analyzing sports scenes, computer vision techniques are also used. In professional tennis matches, one uses the Hawk-eye system(Hawk-Eye, 2002) to judge whether the ball bounces on the court or not. In volleyball matches in Japan, a system that measures a 3-D ball position and shows its trajectory and speed is used.

We are now developing a coaching assist system for tennis players. In this paper, we propose a new method for estimating 3-D trajectories of a tennis ball from multiple video sequences and parameterizing its 3-D trajectories. By using our method, we can stably compute the 3-D ball trajectory and estimate the ball position if we cannot observe it in the input video sequences.

Many researches for tracking a tennis ball and players from video sequences exist. We can classify these methods into two categories. One tracks a tennis ball in 2-D image space. The other estimates the 3-D ball trajectories. Yan et al. proposed a method that tracked a tennis ball from one low quality video(Yan et al., 2005). They extracted a ball region by a frame

difference technique and tracked it by using a particle filter. Archana et al. detected a ball region by a frame difference and background subtraction(Archana and Geetha, 2015). Qazi et al. proposed a method that extracted a ball candidate region by color information and saliency features and decided the ball region by the random forest method(Qazi et al., 2015). Polceanu et al. took a video by a fish-eye lens camera and proposed a method for tracking a tennis ball in real time(Polceanu et al., 2018). All these methods extracted and tracked a ball in the image frames.

On the other hand, Takanohashi et al. proposed a method for reconstructing a 3-D ball trajectory by a shape from silhouette method(Takanohashi et al., 2007). They also reconstructed the 3-D trajectory from asynchronous video sequences. Fazio reconstructed 3-D positions of the ball from two smart phone videos. Since their method reconstructs a ball position by two-view reconstruction, they cannot reconstruct it if the ball is not observed in one or both cameras. Miyata et al. proposed a method that reconstructed a ball trajectory from multi-view videos(Miyata et al., 2017). They automatically synchronize video sequences from uncalibrated and asynchronous video sequences by using an epipolar constraint. However, they assume that a ball is observed in all video sequences. In our research, we reconstruct a 3-D ball position by two-view reconstruction technique among some image pairs. Therefore, our method can reconstruct the ball position if the ball is not observed in some cameras.

^a <https://orcid.org/0000-0003-2831-0054>

^b <https://orcid.org/0000-0002-4400-1051>

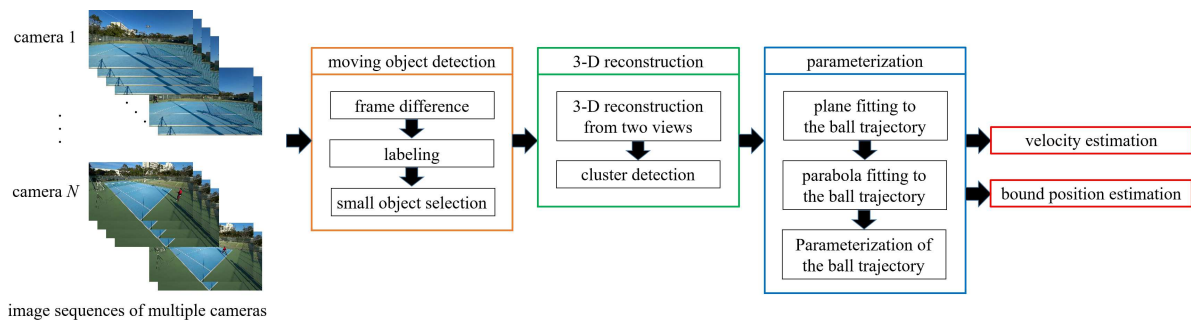


Figure 1: Illustration of our proposed method flow.

2 PROPOSED METHOD

2.1 Overview of the Proposed Method

We propose a new method for estimating 3-D trajectories of a tennis ball from multiple video sequences and parameterizing them by parabola equations. By using the parameterized trajectories, we can estimate the ball speed and its bounced position.

We reconstruct 3-D positions of moving objects, which are extracted by a frame difference technique, by two-view reconstruction and decide the centroid of a cluster points as the position of the ball. After computing a 3-D ball trajectory, we fit a plane to them and express those trajectory as 2-D points. Then, we fit two parabolas to them and correct and interpolate them by the fitted parabola equations.

Therefore, our method has the following advantages against the existing methods and these are the contributions of this paper:

- We can obtain the 3-D ball position without deciding and tracking the 2-D ball position explicitly. This is superior to the tracking based methods.
- We can compute the ball position if we cannot observe it in some images. Miyata's methods uses multiple camera information, however, they assume that a ball is observed in all video sequence.
- We can stably obtain the ball position compared with a multi-view reconstruction by reducing influences of miss-detection and noise of the 2-D ball position.
- By fitting a parabola to a ball trajectory, we can estimate the 3-D ball position and its speed at an arbitrary time.

We show the flow of our proposed method in Fig. 1. We roughly classify all the process into three categories.

1. Ball candidate detection by a frame difference technique

2. 3-D reconstruction of the ball trajectory
3. Parameterization of the ball trajectory

We denote the details of each process in the following sections.

2.2 Preprocessing

We calibrate the camera parameters and synchronize all video sequences in advance. For camera calibration, we capture a chess pattern and estimate the intrinsic parameters of the cameras by Zhang's method (Zhang, 2000). Then, after fixing the cameras around the tennis court, we estimate the extrinsic parameters of the cameras, namely camera location and pose, from the correspondences of 3-D and 2-D line parameters of the tennis court by Zhang (Zhang et al., 2012). For video synchronization, we manually synchronize video sequences by visual inspection. The automatic synchronization of the video sequences is a future work.

2.3 Ball Candidate Region Extraction

For a ball region extraction from an image, we use a well-known techniques for detecting moving objects. We first extract moving objects from video images by using a frame difference technique. For a target image $I^{(t)}$ at a time t , we apply pixel subtraction by $I^{(t-k)}$ and $I^{(t+k)}$ and generate binary images $B^{(t,t-k)}$ and $B^{(t,t+k)}$ by thresholding, respectively. Here, k is a frame interval for the frame difference.

We extract moving objects in $I^{(k)}$ by applying AND operation for the binary images $B^{(t,t-k)}$ and $B^{(t,t+k)}$ followed by morphology operation for noise reduction. Finally, we select centroids of the detected small objects as candidates of a tennis ball position. Here, it is difficult to select a ball among the extracted moving objects. In this process, we do not decide one candidate position.

3 3-D RECONSTRUCTION OF A BALL TRAJECTORY

3.1 Flow of the 3-D Reconstruction

From the extracted candidate ball positions in images, we first make point pairs for all candidate points in all the image frame pairs. Then, we reconstruct 3-D positions of the point pairs by two view reconstruction method if they satisfy the epipolar constraint. We detect cluster points among all the reconstructed points and decide their centroid as a 3-D ball position.

3.2 Epipolar Constraint

For given corresponding points $x^{(1)} = (x^{(1)}, y^{(1)}, 1)^\top$ and $x^{(2)} = (x^{(2)}, y^{(2)}, 1)^\top$ between two images, the following epipolar equation holds:

$$(x^{(1)}, Fx^{(2)}) = 0, \quad (1)$$

where, F is a 3×3 matrix and is called a fundamental matrix. The notation (a, b) shows an inner product of two vectors a and b . For a point pair between two images, we can compute the distances from a point to the epipolar line defined by the other point by changing the roll of two points. We judge that the point pair satisfies the epipolar constraint if the mean distance is small.

3.3 3-D Reconstruction from Feature Points

If we know the matrix $A^{(k)}$ defined from the k -th camera intrinsic parameters and the camera motion $\{R^{(k)}, t^{(k)}\}$, we can reconstruct a 3-D point from $N(N \geq 2)$ correspondences of image points (Hartley and Zisserman, 2004; Kanatani et al., 2016).

In our method, we only detect moving objects in an image space, namely a ball position are identified. Therefore, we first reconstruct a 3-D point from all the detected point pairs if they satisfy the epipolar constraint.

3.4 Decision of the 3-D Ball Position

After reconstructing 3-D points by two-view reconstruction, we detect a cluster among them. For each 3-D point, we count neighboring points whose distance from the target point are smaller than a pre-defined threshold and we regard the point whose neighboring points are maximum and its neighboring points as the cluster points. By considering the consistency between consecutive frames, we detect a cluster

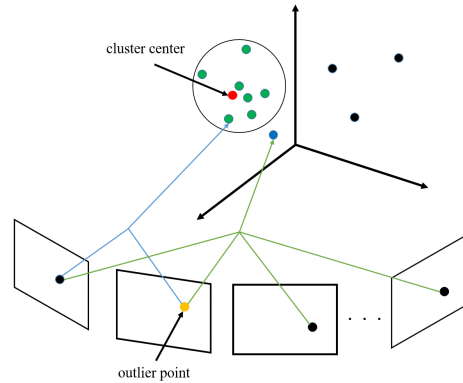


Figure 2: 3-D reconstruction of multi-view reconstruction and cluster center.

which exists near the detected clusters in neighboring frames. Then, we decide the centroid of those cluster points as a 3-D ball position.

This 3-D position is not a reconstructed point from image feature points, however, we consider that the centroid of the cluster points is similar to a point reconstructed by a multi-view reconstruction, because the multi-view reconstruction computes the point so as to minimize the sum of the distances from the lines of view points passing through the feature points. So, we think that if we have no outlier image points, the accuracy of the 3-D points reconstructed from the multi-view reconstruction and the cluster center are almost same. However, if we have outliers from which the reconstructed 3-D points are in the cluster (a yellow point in Fig. 2), the accuracy of 3-D point reconstructed by a multi-view reconstruction may deteriorate (a blue point in Fig. 2).

Therefore, our method has the advantage that we can stably obtain the ball position compared with a multi-view reconstruction by reducing influences of miss-detection and noise of the 2-D ball position. We confirmed this advantage in the experiment section.

4 PARAMETERIZATION OF BALL TRAJECTORY

For parameterizing the computed ball trajectory, we apply the following processes:

1. In order to express the 3-D trajectory points as a 2-D point sequence, we fit a plane to them and project them onto the fitted plane.
2. We fit two parabolas to the 2-D point sequence and express it by parabola equations.

Since a ball trajectory is not a strict parabola shape, we divide the computed trajectory into two

partial data with overlap and fit two parabolas to them, respectively.

3. We correct the observed points and interpolate the missing points by the computed parabola equations.

By parameterizing the ball position for parabola equations, we can estimate a bounce position of the ball if we cannot observe it in images.

4.1 Plane Fitting to the 3-D Trajectory

In order to express a 3-D trajectory of a ball as a 2-D data, we first fit a plane to the 3-D trajectory. A plane equation in 3-D space can be written in the form

$$Ax + By + Cz + D = 0. \quad (2)$$

For 3-D trajectory $r_\alpha = (x_\alpha, y_\alpha, z_\alpha)^\top$, $\alpha = 1, \dots, N$, if we define a data vector $\xi_\alpha = (x_\alpha, y_\alpha, z_\alpha, 1)^\top$ and a parameter vector $u = (A, B, C, D)^\top$, we have $(\xi_\alpha, u) \approx 0$ in the presence of the noise.

The simplest method for computing the plane parameter u is the least squares and the solution is given by minimizing the following function:

$$J = \sum_{\alpha=1}^N (\xi_\alpha, u)^2 = (u, Mu), M = \sum_{\alpha=1}^N \xi_\alpha \xi_\alpha^\top. \quad (3)$$

As we know, the solution of the least squares is given as the unit eigenvector of the smallest eigenvalue of the matrix M . In this paper, by considering the presence of outlier points, we fit a plane in the RANSAC mechanism (Fischler and Bolles, 1981). After computing a plane parameter vector u , we compute a projection matrix P by

$$P = I - nu^\top, \quad n = N[(A, B, C)^\top], \quad (4)$$

where, I is a 3×3 identity matrix and $N[a]$ is a normalization operator that normalizes a vector norm to be 1.

Them, we compute the 3-D data r'_α by projecting the 3-D data r_α onto the plane that is parallel to the fitted plane and passes through the origin as follows:

$$r' = Pr. \quad (5)$$

4.2 Rotation of the Plane

Since we parameterize a ball motion in 2-D space, we need to restore the estimated ball position to a 3-D data. Therefore, we rotate the fitted plane so that the rotated plane is parallel to the YZ plane in the world coordinate system and express the trajectory data as 2-D data in this plane. By this way, we can obtain a 3-D ball position at an arbitrary time by applying inverse rotation for the estimated 2-D position.

For computing such a rotation, we consider a rotation such that the normal vector of the fitted plane and the two vectors that span the plane correspond to the XYZ axes of the world coordinate system.

By applying this rotation to the projected trajectory points, we have the 3-D data whose X values are 0. We select Y and Z values of the 3-D data and express it as 2-D data. Then we use it for a parabola fitting.

4.3 Parabola Fitting to the 2-D Trajectory

In our method, we assume the following parabola equation without rotation.

$$Ax^2 + 2Bx + 2Cy + D = 0. \quad (6)$$

We define a data vector ξ and a parameter vector u in

$$\xi = \begin{pmatrix} x^2 \\ 2x \\ 2y \\ 1 \end{pmatrix}, \quad u = \begin{pmatrix} A \\ B \\ C \\ D \end{pmatrix}, \quad (7)$$

Eq. (6) is written by $(\xi, u) = 0$. Therefore, we can compute the parabola parameter u by the same way of the plane fitting. Moreover, we also apply the RANSAC to a parabola fitting by considering the presence of outlier points.

4.4 Correction and Interpolation of Data

Based on the fitted parabola, we project the observed data onto it and interpolate the missing data, for example, removed points as outliers of a plane and a parabola fitting.

In order to project a 2-D point onto the fitted parabola, we need to compute the its foot of the perpendicular line. However, since it is difficult to compute it analytically, we apply the Sugaya's method (Sugaya, 2010) to the parabola equation defined by Eq. (6). For limitation of the paper space, we omit the details of the algorithm.

We interpolate the missing points linearly by using the corrected points and the fitted parabola equation.

5 EXPERIMENTAL RESULTS

5.1 Simulation for Quantitative Evaluation

We first evaluated the accuracy of the 3-D reconstruction by simulated data. We virtually fixed 16 cameras

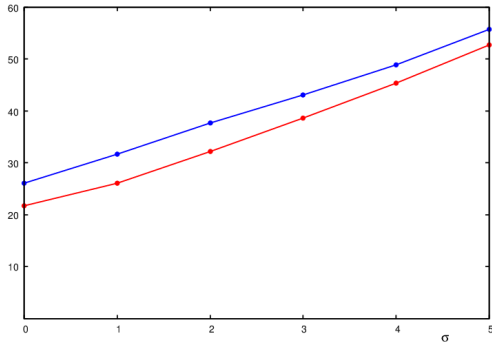


Figure 3: Comparison of 3-D reconstruction error. the blue line: multi-view reconstruction, the red line: the proposed method.

around a tennis court. Their positions are almost same as shown in Fig. 4. We defined the origin of a world coordinate system at the center of the tennis court and set X , Y , and Z axes as red, green and blue line shown in the Fig. 4, respectively. We randomly generated 10000 points in the tennis court space with 3000 mm height, namely, $-5485 \leq x \leq 5485$, $-11885 \leq y \leq 11885$, and $0 \leq z \leq 3000$, in millimeter unit, respectively, and projected them onto the virtual image planes with 1920×1080 pixels. If the projected points were out of the image frame, we judged that we could not observe the ball from these cameras. Then, we added independent Gaussian noise of mean 0 and standard deviation σ , $\sigma = 0.0, 1.0, \dots, 5.0$ to the x and y coordinates of the projected image points. For realizing outlier points, we randomly selected from 0 to 5 cameras and add independent Gaussian noise of mean $5.0 + 2\sigma$ and standard deviation σ , $\sigma = 0.0, 1.0, \dots, 5.0$ to its projected points. Then, we estimated their 3-D positions by the proposed method and a multi-view reconstruction.

Figure 3 shows the average error computed by

$$\frac{1}{N} \sum_{\alpha=1}^N \|\bar{X}^{(\alpha)} - X^{(\alpha)}\|, \quad (8)$$

where $\bar{X}^{(\alpha)}$ and $X^{(\alpha)}$ are the true position and the estimated 3-D position of the α -th point, respectively and N is the number of points. The horizontal axis shows the standard deviation σ for Gaussian noise. In this experiment, we set the threshold for finding a cluster points to be 200 [mm]. From the result of Fig. 3, the proposed method is superior to the multi-view reconstruction.

5.2 Conditions of Real Experiments

We fixed 16 cameras around a tennis court and captured tennis scenes by the SONY FDR-X3000 at 120

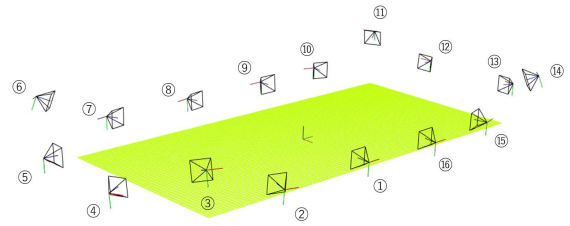


Figure 4: Calibrated camera positions.

fps. The image size is 1920×1080 pixels. We manually calibrated camera extrinsic parameters by 2-D and 3-D line correspondences. Figure 4 shows the calibrated camera positions. We manually synchronized all video sequences and tested our method for the eleven divided partial sequences. We set the threshold for finding a cluster points to be 200 [mm]. For RANSAC, we stop iteration if the solution does not change 200 times consecutively.

5.3 Reconstructed 3-D Ball Trajectories

Figure 5 shows ball candidate points detected by a frame difference. For these candidate points, we made stereo pairs and reconstructed 3-D positions of them if the stereo pairs satisfy the epipolar constraint. The green and red circles in Fig. 5 show the detected candidate points. From Fig. 5, we can see that the moving objects which are not a tennis ball, for example human and its shadow, are also detected. Figure 6 shows the reconstructed 3-D points of the detected moving objects in the 2925-th frame, which is in the 6-th partial sequence. The black points are all the reconstructed points and the green points indicate the selected cluster points, and the red is their centroid. The red circle in Fig. 5 shows the position used by two-view reconstruction of the green cluster points.

We also show the 3-D trajectory of the 6-th partial sequence in Fig. 7. The red line shows the result of our method and the blue line shows the results of a multi-view reconstruction. We used the cluster point, which are the green points in Fig. 6, for the multi-view reconstruction. As you can see, our method gives stable results compared with the multi-view reconstruction. The green point is the 3-D point of the 2925-th frame reconstructed by the multi-view reconstruction. By checking the ball position of the 14-th camera in Fig. 5, we find that the detected ball position is not a correct ball position. From this result, we confirmed the our method could reduce the influence of such a miss detection and obtain a stable result.

We show the reconstructed ball trajectories of all sequences in Fig. 8.

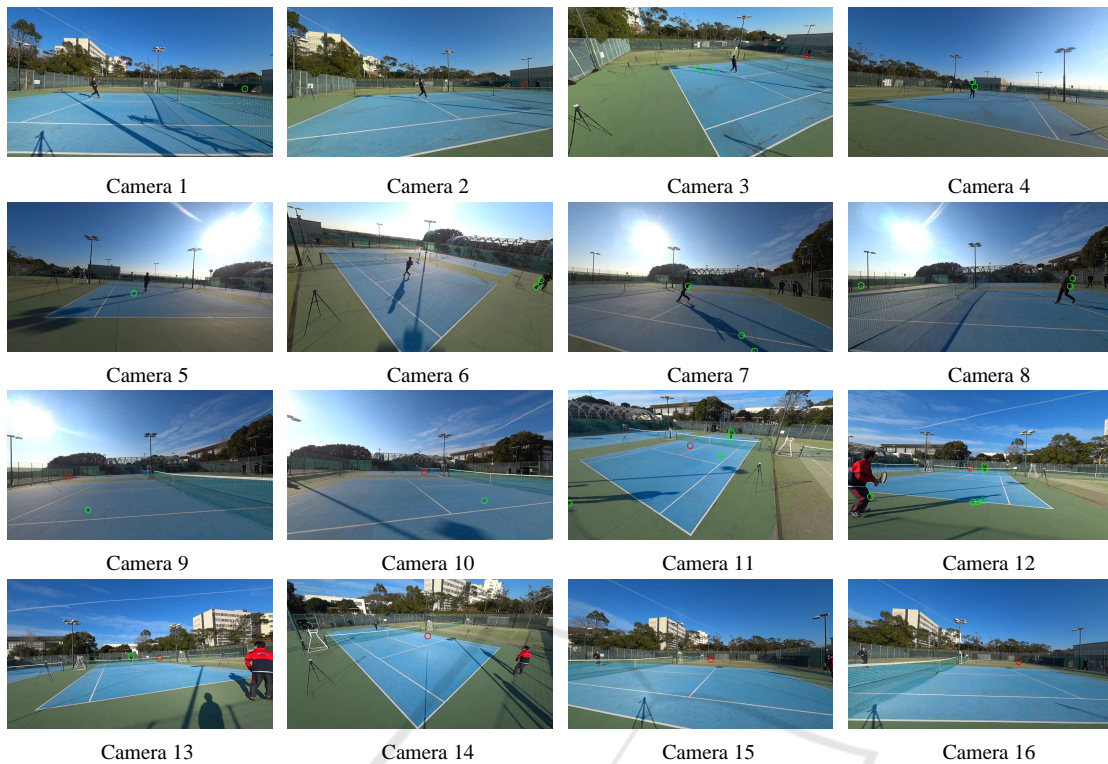


Figure 5: Detected ball candidate points. The center of green circle, including a red circle, indicates a candidate of the ball position extracted by a frame difference. Red circle indicates the ball position used by two-view reconstruction of selected cluster points.

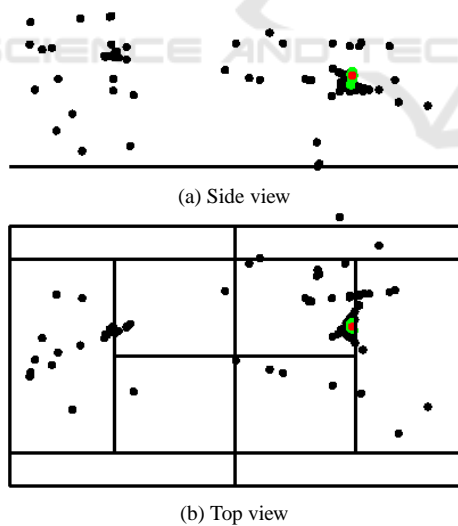


Figure 6: 3-D reconstruction of the ball candidate points. Green points indicate cluster points. Red point indicates centroid of the cluster. Black points indicate the others.

5.4 Results of Ball Trajectory Parameterization

For the computed 3-D trajectories, we manually selected partial trajectories which lie on the first

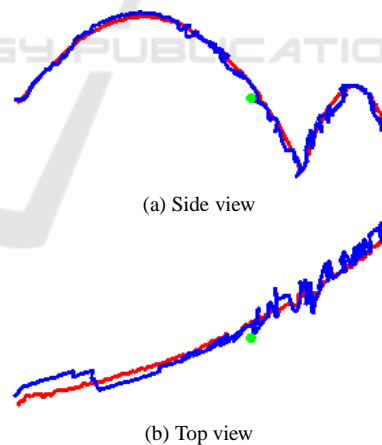


Figure 7: Computed 3-D trajectory. Red line indicates the result of our method. Blue line is the result of a multi-view reconstruction. Green point is the 3-D point of 2925-th frame reconstructed by the multi-view reconstruction.

parabola shape and parameterized them as parabola equations.

We fitted a plane to the estimated 3-D ball trajectory and expressed it as a 2-D point sequence. Next, we fitted two parabolas to the 2-D points and corrected and interpolated them by the fitted parabolas.

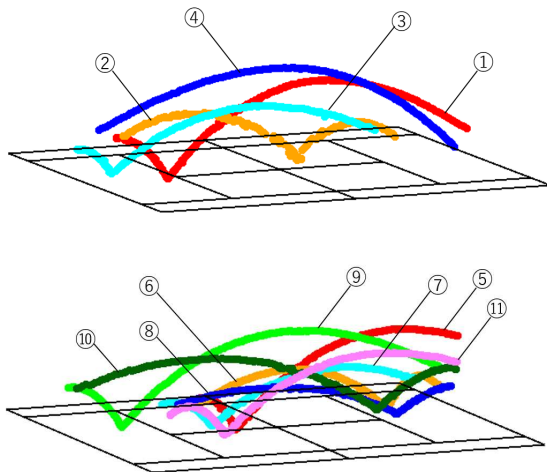


Figure 8: Reconstructed ball trajectories.

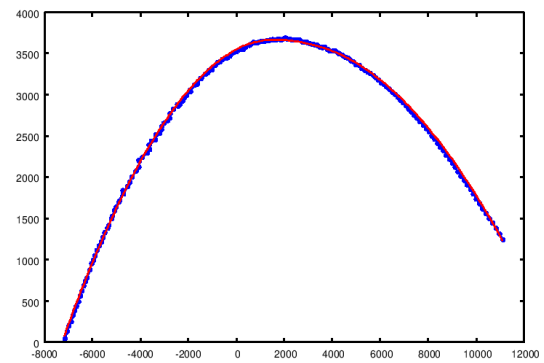
Figure 9 shows the results for the two trajectories (1) and (2) in Fig. 8. The blue points show the input 2-D points computed by a plane fitting and the red points are the result of data correction and interpolation.

Since the input data of Fig. 9(a) is accurately estimated data, outlier points are not detected on the plane fitting and the parabola fitting processes and the result of our method matches to the input data very well. On the other hand, the input data of Fig. 9(b) is very noisy and there exists outlier points. The green points in Fig. 9(b) are the outlier points detected by the parabola fitting. However, the result of our method is very smooth and matches to the input data.

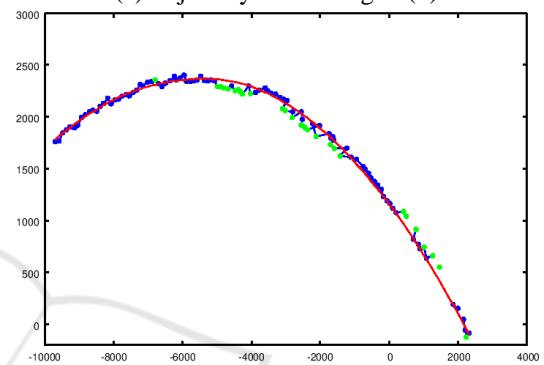
5.5 Estimation of Unobserved Ball Position

Finally, we estimated a bounce position of the ball of the trajectory data (4) in Fig. 8. The last image frame of this sequence corresponds to an immediately before frame that the ball bounces.

Figure 10(a) shows the result of bounce position estimation. The blue points are the observed ball positions in a 2-D space and the red line is the fitted parabola to the latter data of the observed points. The black line corresponds the ground of the world coordinate system. We computed the intersection between the parabola and the ground line. The green point shows the computed intersection. We restored this intersection to the 3-D point in the world coordinate system and obtained the coordinates as $(-1173.88, 11912.33, 0)$. Since the length from the court center to the end line is $11885[\text{mm}]$ in definition and we assume the radius of the ball is $33.5[\text{mm}]$, we will judge that the ball bounces on the court.



(a) trajectory data of Fig. 8 (1)



(b) trajectory data of Fig. 8 (2)

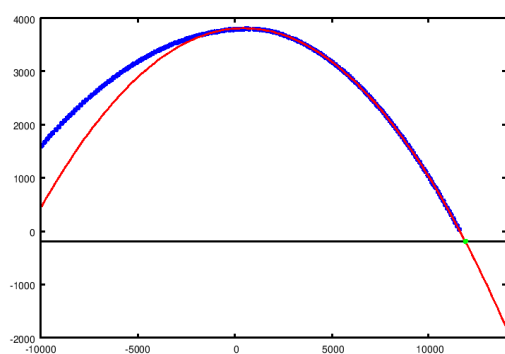
Figure 9: 2-D ball trajectory. Blue points are the computed 2-D ball trajectory obtained from 3-D trajectory. Red points are the corrected and interpolated points by our parabola fitting method.

Figures 10(b) and (c) show the ball positions in the last frame of this trajectory data. We can see that the ball is located near the end line and we do not judge whether the ball bounces in the court or not. The red points are the computed 2-D image position from the estimated 3-D ball positions and the blue point shows the estimated bounce position.

We also estimated un-reconstructed ball positions. Since we set a frame difference parameter k be 2, we could not estimate 3-D positions of the ball in the last two frames. So, we estimated their positions by interpolating them based on the fitted parabola equation. The green points in Figs. 10(b) and (c) show their estimated positions. As we can see that the last green point is drawn on the ball.

6 CONCLUSIONS

We proposed a new method for estimating 3-D trajectories of a tennis ball from multiple video sequences and parameterizing the 3-D trajectories by parabola equations. We reconstructed 3-D ball positions of the



(a) Bounce position estimation in 2-D space.



(b) View from the camera No. 11 in Fig. 4



(c) View from the camera No. 14 in Fig. 4

Figure 10: Bounce position estimation result for the trajectory data of Fig. 8 (4).

extracted candidate 2-D position by two-view reconstruction for every image pairs. By analyzing a distribution of the reconstructed 3-D points, we decided a centroid of the cluster as the 3-D ball position. Moreover, we parameterized the 3-D ball trajectories by fitting two parabolas to them.

In our simulation and real video experiments, we confirmed that our method stably estimated the 3-D ball trajectory compared with a multi-view reconstruction method. We also confirmed that a ball trajectory can be accurately parameterized by simple parabola equations. We also estimated a bounce position by using our parameterization result.

In future works, we plan to tackle automated synchronization of input video sequences by using an epipolar constraint. We also plan that we measure a ball speed by a speed gun and compare it with the speed estimated from our 3-D reconstruction results.

REFERENCES

- Archana, M. and Geetha, M. K. (2015). Object detection and tracking based trajectory in broadcast tennis video. *Procedia Computer Science*, 58:225–232.
- Fischler, M. A. and Bolles, R. C. (1981). Random sample consensus: A paradigm for model fitting with applications to image analysis and automated cartography. In *Communications of the ACM*, volume 24, pages 381–395.
- Hartley, R. and Zisserman, A. (2004). *Multiple View Geometry in computer vision*. Cambridge University Press.
- Hawk-Eye (2002). <http://www.hawkeyeinnovations.co.uk>.
- Kanatani, K., Sugaya, Y., and Kanazawa, Y. (2016). *Guide to 3D Vision Computation: Geometric Analysis and Implementation*. Stringier International.
- Miyata, S., Saito, H., Takahashi, K., Mikami, D., Isogawa, M., and Kimata, H. (2017). Ball 3d trajectory reconstruction without preliminary temporal and geometrical camera calibration. In *IEEE Conference on Computer Vision and Pattern Recognition Workshop*, pages 164–169.
- Polceanu, M., Petac, A. O., Lebsir, H. B., Fiter, B., and Buche, C. (2018). Real time tennis match tracking with low cost equipment. In *The Thirty-First International Florida Artificial Intelligence Research Society Conference (FLAIRS-31)*, pages 197–200.
- Qazi, T., Mukherjee, P., Srivastava, S., Lall, B., and Chauhan, N. R. (2015). Automated ball tracking in tennis videos. In *Third International Conference on Image Information Processing*, pages 236–240.
- Sugaya, Y. (2010). Ellipse detection by combining division and model selection based integration of edge points. In *Proceedings of the 4th Pacific-Rim Symposium on Image and Video Technology*, pages 64–69.
- Takanohashi, K., Manabe, Y., Yasumuro, Y., Imura, M., and Chihara, K. (2007). Measurement of 3d ball trajectory using motion blur. *IPSI Transactions of Computer Vision nad Image Media*, 48(SIG 1):35–47.
- Yan, F., Christman, W., and Kittler, J. (2005). A tennis ball tracking algorithm for automatic annotation of tennis match. In *British Machine Vision Conference 2005*.
- Zhang, X., Sun, X., Yuan, Y., Zhu, Z., and Yu, Q. (2012). Iterative determination of camera pose from line features. In *International Archives of the Photogrammetry, Remote Sensing and Spatial Information Sciences*, volume XXXIX-B1, pages 81–86.
- Zhang, Z. (2000). A flexible new technique for camera calibration. *IEEE Transactions on Pattern Analysis and Machine Intelligence*, 22(11):1330–1334.